Inorg. Chem. **2002**, *41*, 6106–6111

Inorganic Chemistry Article

New Lead Inorganic–Organic Hybrid Microporous and Layered Materials: Synthesis, Properties, and Crystal Structures

Jiang-Gao Mao, Zhike Wang, and Abraham Clearfield*

Department of Chemistry, Texas A&M University, P.O. Box 30012,
College Station, Texas 77843-3255

Received June 12, 2002

Two new lead(II) phosphonates, namely, $Pb_2\{PMIDA\}\cdot 1.5H_2O$ (**1**) ($H_4PMIDA = H_2O_3PCH_2N(CH_2CO_2H)_2$) and Pb-($H_2L$) (**2**) ($H_4L = CH_3N(CH_2PO_3H_2)_2$), have been synthesized by hydrothermal reactions at 150 °C. Complex **1** crystallized in tetragonal $P4_2/n$ with cell dimensions of $a = 17.317(7)$ and $c = 7.507(5)$ Å and $Z = 8$. In complex **1**, Pb(1) is 6-coordinated by chelation in a tetradentate fashion by a PMIDA ligand (3 O, 1 N) and two phosphonate oxygen atoms from neighboring Pb(PMIDA) units in a severely distorted octahedral geometry, whereas Pb(2) is 6-coordinated by 4 carboxylate and 2 phosphonate oxygen atoms also with a severely distorted octahedral environment. These two different types of Pb(II) ions are interconnected through bridging carboxylate and phosphonate groups, resulting in a 3D network with micropores, whose cavity is filled by lattice water molecules interlinked via hydrogen bonds. Each PMIDA ligand bridges with 8 Pb(II) ions (3 Pb(1) and 5 Pb(2)). Complex **2** is orthorhombic, $P2_12_12_1$, with $a = 7.382(5)$, $b = 7.440(6)$, and $c = 30.75(2)$ Å and $Z = 8$. The structure of **2** features a 2D double lead(II) phosphonate layer along the *ab* plane. Each lead(II) ion is 5-coordinated by five phosphonate oxygen atoms from four ligands in a distorted trigonal bipyramid geometry. These double layers are further interconnected via hydrogen bonds between the protonated and uncoordinated phosphonate oxygens along the *c*-axis.

Introduction

The chemistry of metal phosphonates has been an active research area in recent years due to potential applications in the areas of catalysis, ion exchange, proton conductivity, intercalation chemistry, photochemistry, and materials chemistry.[1] These materials also exhibit a variety of structures such as 1D chain, 2D layer, and 3D network with micropores, among which the 2D layer is the most common structural type.[1] Materials with open-framework and microporous structures are expected to find use as hybrid composite materials in electrooptical and sensing applications in the future.[2] Our recent researches show that the extent of the deprotonation on the phosphonic acids and the nature of the metal ions are two important factors that affect the structures of the metal complexes formed. For example, *N*-(phosphonomethyl)iminodiacetic acid (H_4PMIDA) can adopt various kinds of coordination modes under different reaction conditions.[3−6] A mixed phosphate−phosphonate layered zirconium compound was made by reaction of a zirconium salt with a mixture of phosphoric acid and H_4PMIDA solutions.[3] When the above reactions were carried out in the absence of phosphoric acid, a linear chain compound was isolated.[4] In both cases the iminodiacetic moieties are only involved in hydrogen bonding while phosphonate metal coordination forms the chains or layers. Under less acidic conditions, we isolated two novel complexes, $[Co_2(PMIDA)(H_2O)_5]\cdot H_2O$, whose structure contains double layers of Co(II) carboxylate interconnected by layers of Co(II) phospho-

---

* To whom correspondence should be addressed. E-mail: clearfield@mail.chem.tamu.edu.

(1) (a) Stein, E.; Clearfield, A.; Subramanian, M. A. *Solid State Ionics* **1996**, *83*, 113. (b) Alberti, G.; Costantino, U. In *Comprehensive Supramolecular Chemistry*; Lehn, J. M., Ed.; Pergamon-Elsevier Science Ltd.: London, 1996; p 1. (c) Clearfield, A. *Curr. Opin. Solid State Mater. Sci.* **1996**, *1*, 268. (d) Clearfield, A. Metal phosphonate chemistry. In *Progress in Inorganic Chemistry*; Karlin, K. D., Ed.; John Wiley & Sons: New York, 1998; Vol. 47, pp 371−510 (and references herein).

(2) (a) Cheetham, A. K.; Ferey, G.; Loiseau, T. *Angew. Chem., Int. Ed.* **1999**, *38*, 3268. (b) Zhu, J.; Bu, X.; Feng, P.; Strucky, G. D. *J. Am. Chem. Soc.* **2000**, *122*, 11563.

(3) (a) Zhang, B.; Poojary, D. M.; Clearfield, A.; Peng, G.-Z. *Chem. Mater.* **1996**, *8*, 1333. (b) Poojary, D. M.; Clearfield, A. *J. Organomet. Chem.* **1996**, *512*, 237. (c) Poojary, D. M.; Zhang, B.; Clearfield, A. *Angew. Chem., Int. Ed. Engl.* **1994**, *33*, 2324.

(4) Zhang, B.; Poojary, D. M.; Clearfield, A. *Inorg. Chem.* **1998**, *37*, 249.

(5) Mao, J.-G.; Clearfield, A. *Inorg. Chem.* **2002**, *41*, 2319.

(6) Gutschke, S. O. H.; Price, D. J.; Powell, A. K.; Wood, P. T. *Angew. Chem., Int. Ed.* **1999**, *38*, 1088.

10.1021/ic020396a CCC: $22.00

© 2002 American Chemical Society
Published on Web 10/19/2002

nate, and a zinc carboxylate–phosphonate hybrid layered complex, $Zn_2(PMIDA)(CH_3CO_2H)]\cdot 2H_2O$.[5] With the complete deprotonation by adding potassium hydroxide, Wood and co-workers obtained the canted antiferromagnet $\{K_2Co(PMIDA)\}_6\cdot xH_2O$, whose crystal structure features a hexameric ring in the chair conformation.[6] Recently a number of divalent metal phosphonates with *N*-methyliminobis(methylenephosphonate) (H_4L) were structurally characterized in our laboratory. Depending on the extent of deprotonation, these metal complexes have three different types of structures, $M(H_3L)_2\cdot 2H_2O$ (M = Mn, Cd) with a 2D layer structure, $Zn(H_2L)(H_2O)$, whose structure features a double chain, and $Zn_3(HL)_2$ with a 3D network.[7] Tin(II), antimony(III), and lead(II) ions show a coordination chemistry different from that of first-row divalent transition metal ions due to the presence of the lone pair electrons and their larger ionic radius.[8–11] $Pb(HO_3PC_6H_5)_2$ has a layer structure in which the Pb(II) ion is 8-coordinated.[8] The structure of tin(II) phosphonopropionate oxalate features a hybrid open-framework. Tin(II) ions are located at the center of the SnO_3E (E represents the lone pair) tetrahedron and SnO_4E square pyramid, respectively.[9a] The structure of $Sn_2(O_3PCH_3)(C_2O_4)$ comprises a network of vertex-linked truncated square-pyramidal SnO_4 units and tetrahedral O_3PC units which gives rise to three-membered rings; through a three-coordinate oxygen, these rings are linked together forming 1D chains, and such chains are connected together via the oxalate groups forming a 2D layer.[9b] A layered $Sb_2O(CH_3PO_3)_2$ and a tubular $NH_4(SbO)_3(CH_3PO_3)_2$ have been reported recently; the Sb(II) ion in both compounds has a coordination geometry of trigonal pyramidal [SbO_4E] (E represents the "lone pair").[10] Two layered lead(II) nitrilotris(methylene)triphosphonates, $Pb[(H_2O_3PCH_2)N(CH_2PO_3H)_2$ and $Pb_2[(O_3PCH_2N(CH_2PO_3H)_2]\cdot H_2O$,[11] have been synthesized, and their structures are quite different from that of other divalent metal triphosphonates reported in our laboratory, namely, $M(NH(CH_2PO_3H)_3)(H_2O)_3$ (M = Mn, Co, Ni, Zn, Cu, Cd), whose structure features a 1D metal phosphonate chain,[12] and the dehydrated $Mn(NH(CH_2PO_3H)_3$, whose structure is a 3D network.[13] The metal ion in hydrated Mn(II) complexes is octahedraly coordinated by three aqua ligands and three phosphonate oxygen atoms, whereas Mn(II) ion in the nonhydrated complex is five coordinated by five phosphonate oxygen atoms with a distorted square pyramid geometry.[13] Our recent efforts to expand our studies from transition metal(II) complexes of H_4PMIDA and *N*-methyliminobis(methylenephosphonate) (H_4L) to their Pb(II) complexes afforded two novel metal phosphonates, $Pb_2\{PMIDA\}\cdot 1.5H_2O$ (**1**) with a microporous structure and $Pb(H_2L)$ (**2**) with a layered structure; these two types of structures are very different from those of complexes of the divalent transitional metal ions.[3–7] Herein we report their synthesis, characterization, and crystal structures.

Experimental Section

Materials and Methods. Deionized water used in all experiments was purified to a resistivity of 17.6 MΩ cm with a Barnstead Nanopure II system. All other chemicals were of reagent grade quality obtained from commercial sources and used without further purification. The ^{31}P solid MAS NMR spectrum was obtained on a Bruker MSL-300 unit, and H_3PO_4 was used as the ^{31}P standard reference. Elemental analysis data were obtained from Desert Analytics, Tucson, AZ. Thermogravimetric analysis was carried out with a TA 4000 unit, at a heating rate of 10 °C/min under an oxygen atmosphere.

Synthesis of $Pb_2(PMIDA)\cdot 1.5H_2O$ (1). Complex **1**, $Pb_2(O_3PCH_2NH(CH_2COO)_2\cdot 1.5H_2O$, was prepared by hydrothermal reactions. A mixture of 1.0 mmol of lead acetate trihydrate (Aldrich), 1 mmol of *N*-(phosphonomethyl)iminodiacetic acid (Aldrich), 2 mL of 40% tetrabutylammonium hydroxide aqueous solution (Aldrich), and 10 mL of deionized water was heated at 150 °C for 5 days. Colorless prismatic crystals (small) and cubic crystals (large) were isolated. Attempts to determine the structure of the cubic crystal were unsuccessful. X-ray diffraction analysis confirmed the prismatic crystals are complex **1**. ^{31}P MAS solid-state NMR measurements show the chemical shift for the phosphonate group is 22.5 ppm with a small peak at 25.5 ppm. The ratio is 5:1. Anal. Found for **1**: C, 8.87; H, 1.15; N, 2.08; P, 4.53. Calcd: C, 9.03; H, 1.36; N, 2.10; P, 4.66. Apparently the composition of the minor impurity is not too different from that of complex **1**.

Preparation of $Pb(H_2L)$ (2). The diphosphonic acid *N*-methyliminobis(methylenephosphonic acid) (H_4L) was prepared by a Mannich type reaction according to the procedures previously described.[7] Complex **2** was also prepared by hydrothermal reactions. A mixture of 1.0 mmol of lead acetate trihydrate (Aldrich), 1 mmol of *N*-methyliminobis(methylenephosphonic acid) (H_4L), and 10 mL of deionized water was heated at 150 °C for 4 days. Colorless crystalline products of **2** were obtained in ca. 78.5% yield. Anal. Found for **2**: C, 8.35; H, 2.07; N, 3.38; P, 14.43. Calcd: C, 8.49; H, 2.14; N, 3.30; P, 14.60.

Crystal Structure Determination. Single crystals of **1** and **2** were mounted on a Bruker Smart CCD using Mo Kα radiation (λ = 0.710 69 Å) and a graphite monochromator at 110(2) K. The cell constants were indexed from reflections obtained from 60 frames collected with 10 s exposure/frame. A hemisphere of data (1271 frames at 5 cm detector distances) was collected by the narrow-frame method with scan widths of 0.30° in ω and exposure time of 20 s/frame. The first 50 frames were recollected in the end of data collection to assess the stability of the crystal, and it was found that the decay in intensity was less than 1%. The data sets were corrected for the Lorentz factor, polarization, air absorption, and absorption due to variations in the path length through the detector faceplate. An empirical absorption correction based on the ψ scan method was also applied.

The space group was uniquely determined to be $P4_2/n$ (No. 86) for **1** and $P2_12_12_1$ (No. 19) for **2**. The structures were solved using direct methods (SHELXTL) and refined by least-squares methods with atomic coordinates and anisotropic thermal parameters for all

---

(7) (a) Mao, J.-G.; Wang, Z.; Clearfield, A. *Inorg. Chem.* **2002**, *41*, 2334. (b) Mao, J.-G.; Wang, Z.; Clearfield, A. *J. Chem. Soc., Dalton Trans.* **2002**, submitted for publication.

(8) Poojary, D. M.; Zhang, B.; Cabeza, A.; Aranda, M. A. G.; Bruque, S.; Clearfield, A. *J. Mater. Chem.* **1996**, *6*, 639.

(9) (a) Stock, N.; Stucky, G. D.; Cheetham, A. K. *Chem. Commun.* **2000**, 2277. (b) Adair, B.; Natarajan, S.; Cheetham, A. K. *J. Mater. Chem.* **1998**, *8*, 1477.

(10) Adair, B. A.; Guillou, N.; Alvarez, M.; Férey, G.; Cheetham, A. K. *J. Solid State Chem.* **2001**, *162*, 347.

(11) Cabeza, A.; Aranda, M. A. G.; Bruque, S.; Clearfield, A. *J. Mater. Chem.* **1999**, *9*, 571.

(12) Sharma, C. V. K.; Clearfield, A.; Cabeza, A.; Aranda, M. A. G.; Bruque, S. *J. Am. Chem. Soc.* **2001**, *123*, 2885.

(13) Cabeza, A.; Ouyang, X.; Sharma, C. V. K.; Aranda, M. A. G.; Bruque, S.; Clearfield, A. *Inorg. Chem.* **2002**, *41*, 2325.

Table 1. Crystal Data and Structure Refinement for **1** and **2**

param	**1**	**2**
formula	$C_5H_9NO_{8.5}PPb_2$	$C_3H_9NO_6P_2Pb$
fw	664.48	424.24
space group	$P4_2/n$ (No. 86)	$P2_12_12_1$ (No. 19)
a/Å	17.317(7)	7.382(5)
b/Å	17.317(7)	7.440(6)
c/Å	7.507(5)	30.75(2)
V/Å^3	2251.1(19)	1689(2)
Z	8	8
D_{calcd}/g·cm^{-3}	3.921	3.338
μ/mm^{-1}	30.054	20.361
GOF on F^2	1.067	1.049
R1, wR2 ($I > 2\sigma(I)$)[a]	0.0553, 0.1210	0.0298, 0.0638
R1, wR2 (all data)[a]	0.0823, 0.1374	0.0328, 0.0646

[a] $R1 = \Sigma||F_o| - |F_c||/\Sigma|F_o|$; $wR2 = \{\Sigma w[(F_o)^2 - (F_c)^2]^2/\Sigma w[(F_o)^2]^2\}^{1/2}$.

non-hydrogen atoms.[14] All hydrogen atoms were generated geometrically, assigned fixed isotropic thermal parameters, and included in the structure factor calculations. The hydrogen atoms for the lattice water molecules in **1** were not refined. The final difference Fourier maps showed featureless residual peaks of 5.665 (for **1**, 0.06 Å from Pb(1) atom) and 1.041 e Å^{-3} (for **2**, 0.91 Å from Pb(1) atom), respectively. Some of the data collection and refinement parameters are summarized in Table 1. Important bond lengths and angles for the two complexes are listed in Table 2. More details on the crystallographic studies as well as atom displacement parameters are given in the Supporting Information.

Results and Discussion

The structure of **1** is very different from the layered Co(II) and Zn(II) complexes we reported previously,[5] even though they have the same metal/ligand ratio. As shown in Figure 1, the asymmetric structural unit of **1** contains two lead atoms and one PMIDA ligand. Pb(1) is 6-coordinated by a PMIDA ligand in a tetradentate fashion (N(1), O(3), O(2), and O(13)) and two phosphonate oxygen atoms from two neighboring Pb(PMIDA) units. Tetradentate chelation of a metal ion by PMIDA was observed also in the Co(II) and Zn(II) complexes.[5] The coordination geometry around the Pb(1) atom is a severely distorted octahedron; the distortion is mainly due to the presence of the lone pair electrons of the lead(II) ion.[8,11] Pb−O distances range from 2.533(9) to 2.69(1) Å. Pb2 is also 6-coordinated by 4 carboxylate and 2 phosphonate oxygen atoms with a distorted octahedral geometry. The Pb−O distances are in the range of 2.331(9)−2.876(9) Å (Table 2). As shown in Chart 1, the coordination mode of the PMIDA in **1** differs greatly from that in Co(II) and Zn(II) complexes, despite its tetradentate chelating function in all three complexes (Chart 1). In the Zn(II) complex, the carboxylate group and phosphonate group bridge with two and three metal ions, respectively (Chart 1c), whereas in the Co(II) complex one of the two carboxylate groups connects with only one metal ion (Chart 1b).[5] One carboxylate group of PMIDA in **1** adopts an μ_3-chelate and bridging coordination mode, whereas the other one bridges with three different metal ions using a unidentate-coordinated oxgen and a μ_2 bidendate coordinated oxygen atom (Chart 1d). O(12) and O(13) each connect with two Pb(II) ions, whereas O(11) bonds with only one Pb(II) ion; thus, one phosphonate group bridges with five Pb(II) ions.

Table 2. Selected Bond Lengths (Å) and Angles (deg) for **1** and **2**[a]

	Compound **1**		
	Bonds		
Pb(1)−O(13)	2.533(9)	Pb(1)−O(2)	2.551(9)
Pb(1)−N(1)	2.625(11)	Pb(1)−O(12)#1	2.677(9)
Pb(1)−O(3)	2.690(10)	Pb(1)−O(13)#2	2.693(10)
Pb(2)−O(12)#3	2.331(9)	Pb(2)−O(2)#4	2.403(9)
Pb(2)−O(11)#5	2.469(9)	Pb(2)−O(4)	2.553(10)
Pb(2)−O(3)#6	2.693(9)	Pb(2)−O(1)#4	2.876(9)
	Hydrogen Bonds		
O(1W)···O(2W)	2.775	O(1W)···O(2W)#7	2.775
O(1W)···O(2W)#8	2.698	O(1W)···O(2W)#9	2.698
	Angles		
O(13)−Pb(1)−O(2)	117.8(3)	O(13)−Pb(1)−N(1)	71.8(3)
O(2)−Pb(1)−N(1)	63.0(3)	O(13)−Pb(1)−O(12)#1	103.0(3)
O(2)−Pb(1)−O(12)#1	137.6(3)	N(1)−Pb(1)−O(12)#1	125.7(3)
O(13)−Pb(1)−O(3)	90.5(3)	O(2)−Pb(1)−O(3)	102.8(3)
N(1)−Pb(1)−O(3)	62.1(3)	O(12)#1−Pb(1)−O(3)	63.9(3)
O(13)−Pb(1)−O(13)#2	78.7(3)	O(2)−Pb(1)−O(13)#2	80.5(3)
N(1)−Pb(1)−O(13)#2	111.3(3)	O(12)#1−Pb(1)−O(13)# 2	120.7(3)
O(3)−Pb(1)−O(13)#2	168.9(3)	O(12)#3−Pb(2)−O(2)#4	83.4(3)
O(12)#3−Pb(2)−O(11)# 5	71.9(3)	O(2)#4−Pb(2)−O(11)#5	82.6(3)
O(12)#3−Pb(2)−O(4)	82.9(3)	O(2)#4−Pb(2)−O(4)	85.4(3)
O(11)#5−Pb(2)−O(4)	153.1(3)	O(12)#3−Pb(2)−O(3)#6	68.5(3)
O(2)#4−Pb(2)−O(3)#6	151.5(3)	O(11)#5−Pb(2)−O(3)#6	84.2(3)
O(4)−Pb(2)−O(3)#6	95.4(3)		
	Compound **2**		
	Bonds		
Pb(1)−O(21)	2.288(6)	Pb(1)−O(42)	2.371(6)
Pb(1)−O(31)#1	2.491(6)	Pb(1)−O(33)#2	2.513(6)
Pb(1)−O(43)#2	2.893(6)	Pb(2)−O(43)	2.284(6)
Pb(2)−O(23)	2.302(6)	Pb(2)−O(13)#3	2.538(6)
Pb(2)−O(12)#4	2.588(6)	Pb(2)−O(21)#5	2.910(6)
P(1)−O(12)	1.490(6)	P(1)−O(13)	1.525(6)
P(1)−O(11)	1.557(6)	P(2)−O(23)	1.500(6)
P(2)−O(22)	1.521(6)	P(2)−O(21)	1.538(6)
P(3)−O(31)	1.496(6)	P(3)−O(33)	1.522(6)
P(3)−O(32)	1.554(6)	P(4)−O(42)	1.513(6)
P(4)−O(43)	1.516(6)	P(4)−O(41)	1.523(6)
	Hydrogen Bonds		
O(11)···O(22)#6	2.457	O(32)···O(41)#7	2.451
	Angles		
O(21)−Pb(1)−O(42)	98.5(2)	O(21)−Pb(1)−O(31)#1	84.6(2)
O(42)−Pb(1)−O(31)#1	94.5(2)	O(21)−Pb(1)−O(33)#2	77.2(2)
O(42)−Pb(1)−O(33)#2	95.4(2)	O(31)#1−Pb(1)−O(33)# 2	160.3(2)
O(43)−Pb(2)−O(23)	86.5(2)	O(43)−Pb(2)−O(13)#3	78.0(2)
O(23)−Pb(2)−O(13)#3	84.1(2)	O(43)−Pb(2)−O(12)#4	97.8(2)
O(23)−Pb(2)−O(12)#4	95.9(2)	O(13)#3−Pb(2)−O(12)# 4	175.7(2)

[a] Symmetry transformations used to generate equivalent atoms are the following. **1**: #1, $-y + 1/2, x, -z + 1/2$; #2, $y, -x + 1/2, -z + 1/2$; #3, $y - 1/2, -x + 1, z + 1/2$; #4, $y - 1/2, -x + 1, z - 1/2$; #5, $-x, -y + 1, -z$; #6, $-x, -y + 1, -z + 1$; #7, $-x + 3/2, -y + 1/2, z$; #8, $-y + 1, x - 1/2, z - 1/2$; #9, $y + 1/2, -x + 1, z - 1/2$. **2**: #1, $x - 1, y - 1, z$; #2, $x, y - 1, z$; #3, $x, y + 1, z$; #4, $x - 1, y + 1, z$; #5, $x, y + 1, z$; #6, $x + 1/2, -y - 3/2, -z$; #7, $-x + 1, y + 1/2, -z + 1/2$.

The interconnection of Pb(II) ions by bridging carboxylate and phosphonate groups results in a complex 3D network with large tunnels along the c-axis (Figure 2). These tunnels are created by 32-membered rings, each of which is formed by 4 PMIDA and 4 Pb(II) ions (Figure 3). The diameter of the pore is estimated to be slightly larger than 5 Å; thus, it is of the micropore type. These micropores are hydrophilic due to the amine, carboxylate, and phosphonate groups. The cavity of the tunnels is occupied by the lattice water molecules interlinked through hydrogen bonds (Table 2).

---

(14) Sheldrick, G. M. *SHELXTL, Crystallographic Software Package*, version 5.1; Bruker-AXS: Madison, WI, 1998.

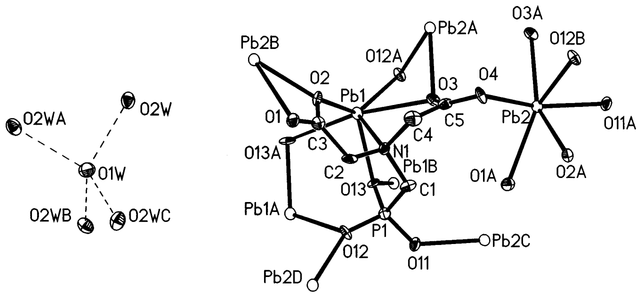

Figure 1. ORTEP representation of the asymmetry unit of complex **1**. Thermal ellipsoids are drawn at 50% probability. The dotted lines indicate hydrogen bonds in the water cluster within the tunnels.

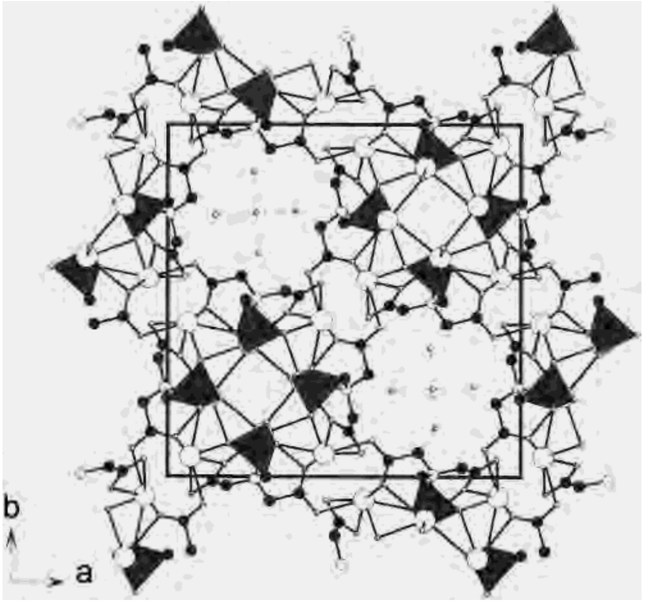

Figure 2. View of structure of complex **1** along the *c*-axis showing the micropores. $C-PO_3$ tetrahedra are shaded in black. Pb, N, C, and O atoms are shown as open (large), open (small), black, and crossed circles, respectively.

Chart 1. H_4PMIDA and Its Coordination Modes in Its Layered Co(II), Zn(II), and Microporous Pb(II) Complexes

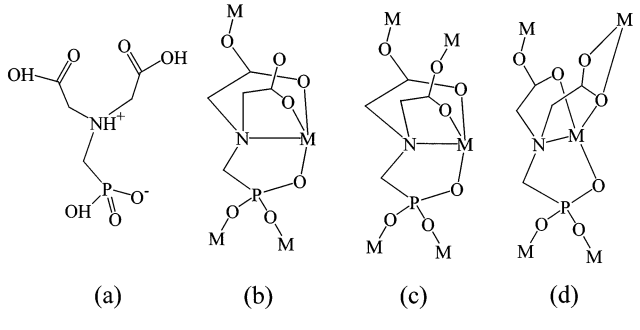

OW1 sits on a mirror plane hydrogen-bonded to four OW2 water molecules tetrahedrally disposed about OW1.

We have reported a number of divalent metal complexes with *N*-methyliminobis(methylenephosphonic acid) (H_4L). They have three different types of structures, namely, $Zn(H_2L)(H_2O)$ with a 1D double chain structure,[7b] $M(H_3L)_2 \cdot 2H_2O$ (M = Cd, Mn) with a 2D layered structure,[7a,b] and $Zn_3(HL)_2$ with a 3D network structure.[7a] The structure of compound **2** features a double layer structure. It has a close relationship with the structure of $Zn(H_2L)(H_2O)$ which will

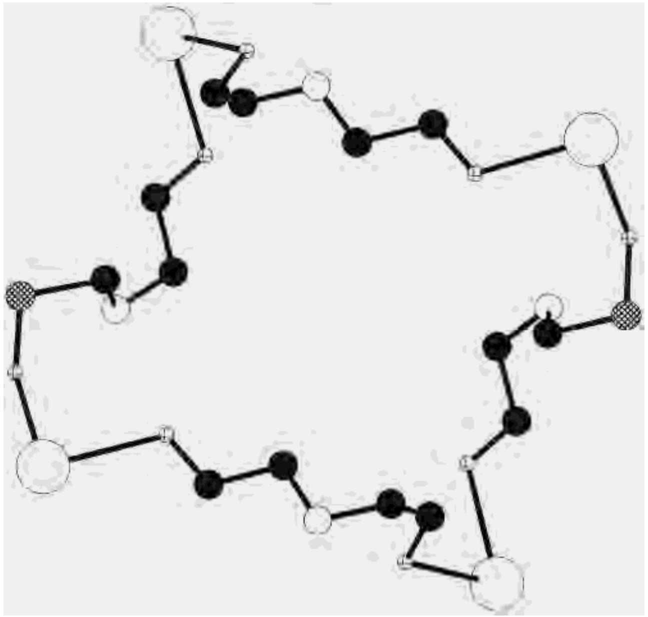

Figure 3. One 32-membered ring formed by 4 PMIDA ligands and 4 Pb atoms in complex **1**. Pb, P N, C, and O atoms are represented by large (open), medium (hatched), medium (open), medium (black), and small (crossed) circles, respectively.

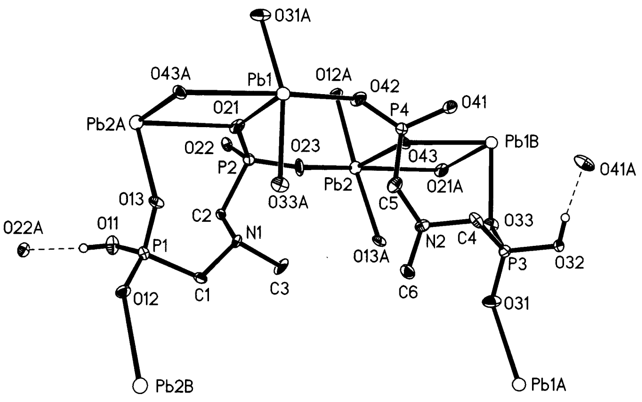

Figure 4. ORTEP representation of the asymmetry unit of complex **2**. Thermal ellipsoids are drawn at 50% probability. The dashed lines represent hydrogen bonds.

be discussed in detail later. As shown in Figure 4, the asymmetric unit of **2** contains two $Pb(H_2L)$ units; each Pb(II) ion is 5-coordinated by five phosphonate oxygen atoms of four different ligands, one of which chelates with the lead(II) ion in a bidentate mode, forming an eight-membered ring (Pb(2a)−O(21)−P(2)−C(2)−N(1)−C(1)−P(1)−O(13) or Pb(1b)−O(33)−P(3)−C(4)−N(2)−C(5)−P(4)−O(43)) (Figure 4). In addition, two of the oxygen atoms in the eight-membered rings, O(21) and O(43), bridge two Pb atoms forming four-membered rings. Each of these oxygens form long and short bonds to Pb as shown in Table 2. Pb(1)−O(43) (2.893(6) Å) and Pb(2)−O21 (2.910(6) Å) distances are much larger than the remaining Pb−O distances (ranging from 2.288(6) to 2.588(6) Å) (Table 2); thus, they are much weaker bonds. The coordination geometry around the Pb(II) ion can be seen as a distorted trigonal bipyramid or a distorted octahedron with an apex occupied by the lone pair of the Pb(II) ion (Figure 4). Similar to that in $Zn(H_2L)(H_2O)$, each pair of metal ions is bridged by a pair of bridging

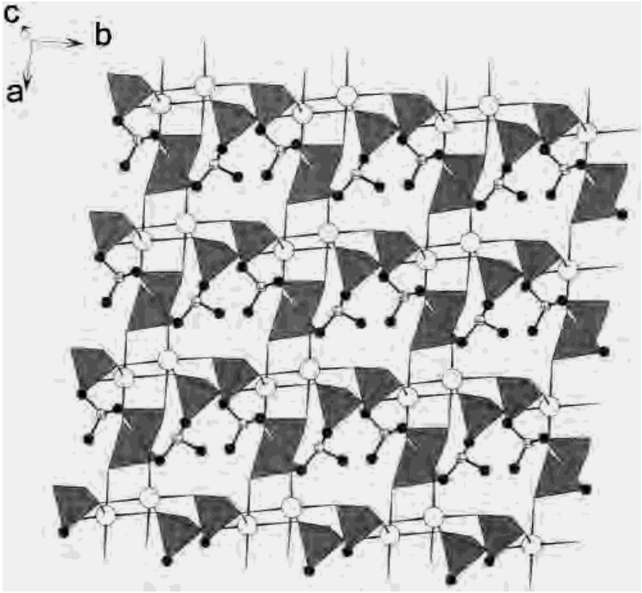

Figure 5. Double layer of complex **2** parallel to the *ab* plane. The phosphonate groups are represented by gray tetrahedra. Pb, N, and C atoms are shown as open (large), crossed, and black circles, respectively.

Chart 2. Ligand H_4L and Its Coordination Modes in Its Metal Phosphonates

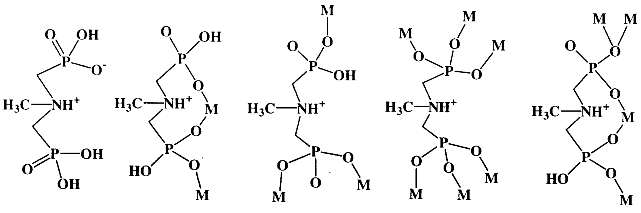

(a) (b) (c) (d) (e)

phosphonate groups, forming eight-membered rings (such as Pb(1)−O(21)−P(2)−O(23)−Pb(2)−O(43)−P(4)−O(42)). These dimeric units are further interconnected by a pair of phosphonate oxygen atoms (such as O(21) and O(43a)) with long Pb−O distances along the *b*-axis and by organic groups along the *a*-axis, resulting in a complicated double layer parallel to the *ab* plane (Figure 5). In the structure of Zn(H_2L)(H_2O), the condensation of the double chains into a 2D layer is terminated by an aqua ligand. Another reason for the termination of the condensation is that the coordination number of the Zn(II) ion is smaller than that of the Pb(II) ion. Similar to that in Zn(H_2L)(H_2O), each ligand in **2** carries two negative charges; one phosphonate group is deprotonated completely, whereas the other one and the nitrogen atom remain 1H-protonated. On the basis of the P−O distances, O(11) and O(32) are most likely to be protonated. The 1H-protonated phosphonate group bridges with two lead(II) ions, whereas the nonprotonated one connects with three Pb(II) ion. O(21) and O(43) atoms each bridge with two Pb(II) ions. This type of μ_2 bridging of oxygen atoms has also been found in complex **1** (Figure 1). The coordination mode of the ligand in complex **2** is different from three other modes we found previously (Chart 2).[7] In layered $M(H_3L)_2 \cdot 2H_2O$ (M = Mn, Cd), each phosphonate group is 1H-protonated; the ligand chelates with a metal ion and bridges with another metal ion (Chart 2b). In the Zn(H_2L)(H_2O) complex, which has a 1D chain structure, one more proton is removed from a phosphonate group and the double-negative charged ligand connects with three different metal ions, one phosphonate group unidentate and the other one in a bidentate fashion. With all protons removed from the phosphonate groups, the resultant three negatively charged ligands in $Zn_3(HL)_2$, whose structure features a 3D network, bridges with 6-different metal ions. O(11), O(22), O(32), and O(41) phosphonate oxygen atoms in complex **2** are not coordinated to the metal ions; however, they are involved in hydrogen bonding. These hydrogen bonds are very strong, having O···O contacts less than 2.50 Å (Table 2). Hydrogen bonds between protonated and uncoordinated phosphonate oxygen atoms further interconnect the double layers along the *c*-axis (Figure 6).

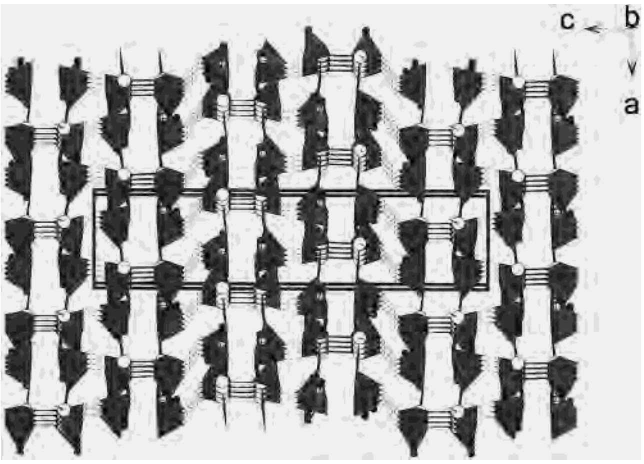

Figure 6. View of structure of complex **2** along the *b*-axis showing the lead diphosphonate double layer parallel to the *ab* plane being interconnected by hydrogen bonds between protonated and uncoordinated phosphonate oxygen atoms. $C-PO_3$ tetrahedra are shaded in gray. Pb, N, and C atoms are shown as open (large), crossed, and black circles, respectively. The dotted lines represent hydrogen bonds.

Compound **1** lost its water of hydration below 100 °C. A TGA curve run with the dehydrated product showed no weight loss to 315 °C, followed by a sharp weight loss of 18.08% to 408 °C. The final weight loss was 18.15% at 1005 °C. An X-ray powder pattern showed the presence of PbO and $Pb_2P_2O_7$. On the assumption that the ratio of products was $^1/_2Pb_2P_2O_7 + PbO$, the total weight loss expected is 18.84% in excellent agreement with the observed value. The ready loss of water without collapse of the structure indicates that the tunnel may readily sorb small polar molecules. This supposition is under examination.

Compound **2** contains no water so it is not surprising that no weight loss occurred until 320 °C even though the flowing gas was O_2. At this temperature decomposition of the compound takes place in a multistep process. Presumably, the first step is the split out of H_2O utilizing the phosphonate group protons. The final product was PbP_2O_7 indicating that the Pb(II) was oxidized to Pb(IV). There is an observed weight gain from 506 to ~750 °C, and the total weight loss was 10.03%. The calculated weight loss is 10.16%. Under an atmosphere of nitrogen the final product should be Pb(PO_3)$_2$, which requires a total weight loss of 13.93%. Presumably, this metaphosphate forms during the decomposition of the compound followed by a slow oxidation to the pyrophosphate.

Acknowledgment. We acknowledge with thanks the financial support from the Robert A. Welch Foundation through Grant No. A673 and the Department of Energy, Basic Sciences Division, through Grant No. DOE 448071-00001.

Supporting Information Available: X-ray crystallographic files in CIF format and tables of X-ray data for the structure determinations of $Pb(O_3PCH_3)$ (**1**), $Pb_2\{PMIDA\}\cdot 1.5H_2O$ (**2**), and $Pb(H_2L)$ (**3**). This material is available free of charge via the Internet at http://pubs.acs.org.

IC020396A